Constellation Design for Media-based Modulation using Block Codes and Squaring Construction

Bharath Shamasundar and A. Chockalingam
Department of ECE, Indian Institute of Science, Bangalore

***Abstract*—Efficient constellation design is important for improving performance in communication systems. The problem of multidimensional constellation design has been studied extensively in the literature in the context of multidimensional coded modulation and space-time coded MIMO systems. Such constellations are formally called as lattice codes, where a finite set of points from a certain high dimensional lattice is chosen based on some criteria. In this paper, we consider the problem of constellation/signal set design for media-based modulation (MBM), a recent MIMO channel modulation scheme with promising theoretical and practical benefits. Constellation design for MBM is fundamentally different from those for multidimensional coded modulation and conventional MIMO systems mainly because of the inherent sparse structure of the MBM signal vectors. Specifically, we need a *structured sparse lattice code* with good distance properties. In this work, we show that using an (N, K) non-binary block code in conjunction with the lattice based multilevel squaring construction, it is possible to systematically construct a signal set for MBM with certain guaranteed minimum distance. The MBM signal set obtained using the proposed construction is shown to achieve significantly improved bit error performance compared to conventional MBM signal set. In particular, the proposed signal set is found to achieve higher diversity slopes in the low-to-moderate SNR regime.**

***Index Terms*—Media-based modulation, mirror activation pattern, MAP-index coding, squaring construction.**

I. Introduction

Media-based modulation (MBM) is a recent MIMO transmission technique which uses a single transmit radio frequency (RF) chain and multiple RF radiation elements. It has compact overall structure compared to the conventional MIMO systems and achieves superior rate and performance [1]-[11]. Specifically, MBM uses digitally controlled parasitic elements called RF mirrors, which act as signal scatterers in the near field of the transmit antenna (see Fig. 1). Each of these RF mirrors can be in one of the two states, namely, ON or OFF, based on the control inputs which depend on the information bits. An RF mirror reflects the transmit signal in the ON state, and allows the signal to pass through in the OFF state. If there are m_{rf} RF mirrors, then there are $N_m \triangleq 2^{m_{rf}}$ different ON/OFF combinations, called 'mirror activation patterns' (MAP). Each of these MAPs creates a different near field geometry for the transmit signals. In a rich scattering environment, even a small perturbation in the near field will be augmented by random reflections, and hence results in a different end-to-end channel. Therefore, in MBM, using m_{rf} RF mirrors, N_m independent channels can be created corresponding to N_m different MAPs. These different MAPs can be represented by the N_m MAP indices, $\mathcal{M} = \{0, 1, \cdots, N_m - 1\}$. The transmitter activates one of these MAPs (equivalently, selects one of the indices from $\mathcal{M}$) based on m_{rf} information bits and transmits a symbol from a conventional modulation alphabet $\mathbb{A}$ (say, QAM), which conveys $\log_2 |\mathbb{A}|$ bits. The achieved rate in MBM is, therefore, given by $\eta_{\text{MBM}} = m_{rf} + \log_2 |\mathbb{A}|$ bits per channel use (bpcu). It has been shown that MBM can achieve good bit error performance in the point-to-point setting compared to conventional SIMO/MIMO systems [1]-[5]. In [6], MBM is studied in the context of space-time coding and significant performance gains are reported. Inspired by the notion of quadrature spatial modulation, quadrature channel modulation schemes using MBM are proposed in [7],[8]. In [9], MBM is used for the uplink in massive MIMO systems, and the possible gains in terms of reduction in the required number of base station receive antennas are highlighted. Recently, practical implementation of MBM using reconfigurable metasurfaces to alter the near-field radiation characteristics have been proposed in [10],[11]. Our new contribution in the present work is on designing efficient signal sets for MBM that can achieve significantly improved system performance.

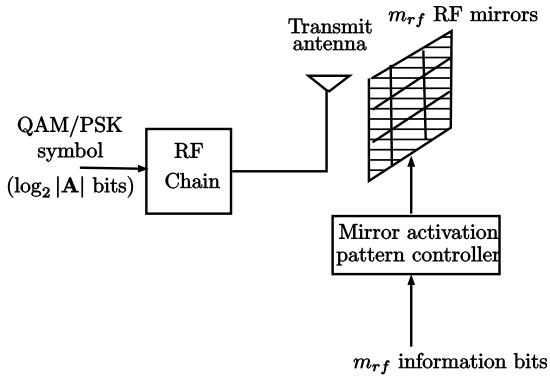

Fig. 1: Schematic representation of MBM transmitter.

Constellation design is one of the important means to improve performance in wireless communication systems. In early literature on constellation design, several two-dimensional constellations are conceived based on different criteria [12]-[14]. Recognizing the limited SNR gains achievable by two-dimensional constellations and the possibility of higher SNR efficiency by going for higher dimensions,

This work was supported in part by the Visvesvaraya PhD Scheme of the Ministry of Electronics & IT, Government of India, J. C. Bose National Fellowship, Department of Science and Technology, Government of India, and the Intel India Faculty Excellence Program.

efficient multidimensional constellations are proposed in the literature [15]-[17]. The general framework of constellation design is formalized by defining the notion of a lattice code, and several efficient methods for constructing lattice codes are presented in the literature in the context of multidimensional coded modulation and MIMO systems [15]-[22]. In the present work, we consider the problem of constellation design for MBM, which is a recently proposed MIMO channel modulation scheme, described briefly in the earlier part of this section. The constellation design for MBM is fundamentally different from those described above mainly because of the sparse nature of the MBM signal vectors. Although some techniques can be borrowed from the previous literature, only marginal gains are possible if sparsity is not explicitly taken into account while designing the constellation. Specifically, we need good *structured sparse lattice codes* in higher dimensions to achieve high SNR efficiency in MBM. To this end, the contributions of this paper can be summarized as follows.

- The problem of constellation design with constraints on the sparsity of signal vectors has not been addressed in the conventional MIMO literature. Since the sparsity arises naturally in MBM, we formulate the constellation design problem for MBM by explicitly considering the sparsity constraints to achieve improved distance properties. Specifically, we consider the design of structured sparse multidimensional constellation, where the elements of the constellation are the joint MBM vectors to be transmitted in N channel uses, i.e., MBM blocks formed by concatenating N MBM vectors.
- Next, we show that using non-binary block codes [23] in conjunction with the lattice based constructions [18],[19], it is possible to design constellation (signal set[1]) for MBM with superior distance properties. We give one such construction of the MBM signal set using the notions of *MAP-index coding* and *multilevel squaring construction*.
- We derive upper bound on the bit error rate (BER) and the asymptotic diversity gain achieved by MBM using the proposed signal set, both of which are verified by simulations.
- Finally, we present simulation results that demonstrate the SNR gain achieved by the proposed signal set. For example, an MBM system of rate 3 bpcu using the proposed signal set achieves a BER of 10^{-4} at an SNR of 6 dB, while the conventional MBM signal set requires 12 dB to achieve the same BER performance. The improved distance properties of the proposed signal set are also numerically demonstrated.

The rest of the paper is organized as follows. Section II provides the necessary preliminaries for the squaring construction, which is used in the latter section for MBM signal set design. The formulation of the signal set design problem, the proposed signal set, and its distance properties are presented in Sec. III. The BER upper bound and the diversity analysis of MBM using the proposed signal set are presented in Sec. IV. Results and discussions are presented in V, and conclusions are presented in Sec. VI.

[1]The terms constellation and signal set are interchangeably used in the paper.

II. Preliminaries

In this section, we present the notions of partitions, partition chains, partition distance lemma, and the squaring construction [18],[19]. These notions will be used in the next section for the MBM constellation design.

Consider a discrete, finite set S. An M-way *partition* of the set S is specified by M disjoint sets $T(b)$, such that their union is the set S. Here, b is the *label* for the subset $T(b)$, which uniquely identifies the subset. This can be an integer labeling, in which case b can take values $0, 1, \cdots, M-1$. If $M = 2^K$, for some $K \in \mathbb{Z}_+$, then we can use binary labelings of K bits. The partition of S into $T(b)$ is denoted by S/T, with the *order* of partition $|S/T| = M$. For example, consider the set $S = \{-4, -3, \cdots, 0, \cdots, 3, 4, 5\}$, which is a subset of integers. A two way partition of this set into odd and even integers is $T(0) = \{-3, -1, 1, 3, 5\}$ and $T(1) = \{-4, -2, 0, 2, 4\}$. The order of partition here is $|S/T| = 2$.

An m-level partition is denoted by $S_0/S_1/\cdots/S_m$ and is obtained by first partitioning S_0 into $S_1(b_0), b_0 = 0, \cdots, M_1 - 1$, then partitioning each $S_1(b_0)$ into $S_2(b_1), b_1 = 1, \cdots, M_2 - 1$, and so on. Here, M_1 is the order of the partition S_0/S_1, M_2 is the order of the partition S_1/S_2, and so on. An m-level partition is generally labeled using m-part label $\mathbf{b} = (b_0, b_1, \cdots, b_m)$, where b_j is the label for the partition S_j/S_{j+1}. In other words, specifying the m-level partition $\mathbf{b}$ uniquely identifies a set from the partition $S_0/S_1/\cdots/S_m$. Further, the subsets at jth level are identified by the first j parts of the label $(b_0, \cdots, b_j)$. If $|S_0/S_1| = M_1$, $|S_1/S_2| = M_2, \cdots$, $|S_{m-1}/S_m| = M_m$, then the order of partition S_0/S_m is the product of the orders at each level, i.e., $|S_0/S_m| = M_1 M_2 \cdots M_m$. For example, if $|S_0/S_1| = 2$ and $|S_1/S_2| = 3$, then $|S_0/S_2| = 2 \cdot 3 = 6$.

Another important notion is that of a *distance* metric defined on a discrete set. If s and s' are two elements of S, then the distance between them is denoted by $d(s, s')$, which is equal to zero only if $s = s'$ and greater than zero otherwise. The *minimum distance* of the set, denoted by $d(S)$, is the minimum $d(s, s')$ for $s \neq s'$. For a partition S/T, the distance metric of S carries over to its subsets $T(b)$. The minimum distance of the partitioned sets $T(b)$ is defined as the least minimum distance among $d(T(b))$. In the present work, we are interested in the partition S/T such that $d(T) > d(S)$. If $T(b)$ and $T(b')$ are subsets of S, then the *minimum subset distance* $d(b, b')$ is equal to $d(T(b))$ if $b' = b$, otherwise, $d(b, b')$ is the minimum distance between the distinct elements of the subsets $T(b)$ and $T(b')$. We now state an important result known as the *partition distance lemma*, which gives the lower bound on the distance between any two subsets in an m-level partition chain.

Lemma II.1. *If $S_0/S_1/\cdots/S_m$ is an m-level partition chain with distances $d(S_0)/d(S_1)/\cdots/d(S_m)$, and $S_m(\mathbf{b})$ and $S_m(\mathbf{b}')$ are subsets with multipart labels $\mathbf{b}$ and $\mathbf{b}'$, respectively, then the subset distance $d(\mathbf{b}, \mathbf{b}')$ is lower bounded by $d(S_j)$, where if $\mathbf{b} \neq \mathbf{b}'$, j is the smallest index such that $b_j \neq b'_j$, while if $b = b'$, j is equal to m.*

This result can be visualized in the form of a binary tree, where the multipart labels are associated with different branches of the tree and the distance between any two subsets depends on which stage the two subsets diverge in the binary tree.

In general, a distance measure is useful if it has *additivity property*. Specifically, if S is a set of N-dimensional vectors $\mathbf{s} \in S$, then the additive property of the distance requires that the distance between any two vectors $\mathbf{s}$ and $\mathbf{s}'$ in S is equal to the sum of distances between each of their components s_i and s'_i, $i = 1, \cdots, N$. It is well known that the squared Euclidean distance naturally has the additive property.

We now present the idea of *squaring construction*, which gives a method of constructing new sets from a given set such that the constructed sets ensure a certain minimum distance greater than that of the set we start with. The squaring construction can be described as follows.

If S is a disjoint union of M subsets $T(b), b = 0, \cdots, M-1$, then the squaring construction is defined as the union of the Cartesian product sets $T(b) \times T(b) = T^2(b)$, $b = 0, \cdots, M-1$, i.e., $U = \bigcup_{b=0}^{M-1} T^2(b)$, which is denoted by $|S/T|^2$. For example, if $S = \{0, 1, 2, 3\}$, $T(0) = \{0, 2\}$, and $T(1) = \{1, 3\}$, then the squaring construction is the union of sets

$$U_1 = T(0) \times T(0) = \{(0,0), (0,2), (2,0), (2,2)\}$$
$$U_2 = T(1) \times T(1) = \{(1,1), (1,3), (3,1), (3,3)\},$$

and the union is

$$U = U_1 \cup U_2 = \{(0,0), (0,2), (2,0), (2,2), (1,1), (1,3), (3,1), (3,3)\}.$$

Note that the set U is a subset of the Cartesian product of S with itself, i.e., $U \subset S \times S$. The following lemma gives an important property of such a construction. Specifically, it says that the squaring construction ensures an increased minimum distance [19].

Lemma II.2. *If S/T is a partition with minimum distances $d(S)/d(T)$, then $U = |S/T|^2$ has a minimum distance of*

$$d(U) = \min\left[d(T), 2d(S)\right]. \tag{1}$$

Proof: Case 1: If two distinct elements of U belong to the same set $T^2(b)$, then they differ in at least one coordinate, and hence have a distance of $d(T)$.
Case 2: If two distinct elements of U belong to different $T^2(b)$s, then the two elements differ in both the coordinates, and hence have a minimum distance of $d(S)$ in each coordinate and $2d(S)$ in total. ∎

Consider the previous example with squared Euclidean distance as the distance measure on S. With this distance measure, the minimum distance of S, $d(S) = 1$. The minimum distances $d(T(0))$ and $d(T(1))$ are both equal to 4. Further, the minimum distance of the set U obtained by squaring construction, $d(U) = 2 = 2d(S)$. Thus, using squaring construction, the minimum distance is increased from one to two. In the process, the dimension of the elements of the set S, which is one, is also increased in U to two.

The squaring construction can be continued iteratively on the resulting sets to construct new sets with their elements in higher dimensions having higher minimum distance. Such a construction is called as the *multilevel squaring construction* or *iterated squaring construction*. It is interesting to note that the idea of squaring construction can be used to construct many good codes and lattices, specifically, Reed-Muller codes and the Barnes-Wall lattices, owing to its elegant way of increasing the distances iteratively. We use this idea of multilevel squaring construction in the next section in conjunction with non-binary block codes to construct an MBM signal set/constellation with very good distance properties.

III. MBM SIGNAL SET DESIGN

In this section, we briefly review MBM system and conventional MBM signal set. We formulate the MBM signal set design problem by imposing certain conditions, which when satisfied can lead to improved distance properties. We propose the technique of MAP-index coding using non-binary block codes in conjunction with multilevel squaring construction (discussed in the previous section) to meet the imposed conditions.

A. Conventional MBM signal set

Consider an MBM system with a single transmit antenna and m_{rf} RF mirrors placed near the transmit antenna. Then, $N_m = 2^{m_{rf}}$ MAPs are possible. Each of these MAPs create different end-to-end channel between the transmitter and the receiver. Let the N_m different MAPs be assigned indices from the set $\mathcal{M} = \{0, 1, 2, \cdots, N_m - 1\}$. An example mapping between the elements in $\mathcal{M}$ and the MAPs for $m_{rf} = 2$ (i.e., $N_m = 4$) is shown in Table I.

Mirror 1 status	Mirror 2 status	MAP index
ON	ON	0
ON	OFF	1
OFF	ON	2
OFF	OFF	3

TABLE I: Mapping of mirror activation patterns to indices.

In a given channel use, one of the MAPs is selected based on m_{rf} information bits and a symbol from a conventional modulation alphabet $\mathbb{A}$ is transmitted using the selected MAP. Let $\mathbb{A}_0 \triangleq \mathbb{A} \cup \{0\}$. Then, the conventional MBM signal set, $\mathbb{S}_{\text{MBM}}$, is the set of $N_m \times 1$-sized signal vectors given by

$$\mathbb{S}_{\text{MBM}} = \big\{\mathbf{s}_k \in \mathbb{A}_0^{N_m},\ \forall k \in \mathcal{M},\ \text{s.t. } \mathbf{s}_k = [0 \cdots 0 \underbrace{x}_{(k+1)\text{th index}} 0 \cdots 0]^T,\ x \in \mathbb{A}\big\}. \tag{2}$$

Consider two MBM signal vectors

$$\mathbf{x}_1 = \begin{bmatrix} 0 \\ \vdots \\ s_1 \\ 0 \\ \vdots \\ 0 \end{bmatrix}, \quad \mathbf{x}_2 = \begin{bmatrix} 0 \\ s_2 \\ \vdots \\ 0 \\ \vdots \\ 0 \end{bmatrix}. \tag{3}$$

The squared Euclidean distance between these two MBM signal vectors is $|s_1|^2 + |s_2|^2$ if the positions of the non-zeros s_1 and s_2 are different, i.e., if $\mathbf{x}_1$ and $\mathbf{x}_2$ have different MAP

indices. On the other hand, if the positions of the non-zeros s_1 and s_2 are the same, i.e., if $\mathbf{x}_1$ and $\mathbf{x}_2$ have the same MAP-index, then the distance is $|s_1 - s_2|^2$. The minimum (squared Euclidean) distance of the conventional MBM signal set, $d(\mathbb{S}_{\text{MBM}})$ is then given by

$$d(\mathbb{S}_{\text{MBM}}) = \min_{s_1, s_2 \in \mathbb{A}} \{|s_1|^2 + |s_2|^2, |s_1 - s_2|^2\}. \tag{4}$$

For example, with the BPSK modulation, the minimum distance $d(\mathbb{S}_{\text{MBM}}) = 2$, irrespective of the number of RF mirrors used.

B. Efficient signal set design for MBM

As just illustrated, the minimum distance between the MBM signal vectors is decided by the modulation alphabet, irrespective of the number of RF mirrors used. Therefore, as such, the distance properties of MBM can not be improved much except for possible marginal improvements achievable by the constellation shaping to make the alphabet $\mathbb{A}$ near-circular [14]. Therefore, we now take a different approach where we form a new constellation with its points being the joint MBM vectors to be transmitted in N channel uses. That is, we consider block transmission of MBM, where a block of N MBM vectors is considered as the constellation point to be transmitted in N channel uses. This is the approach taken in [15]-[17] to construct good constellations in the case of conventional modulation. As we show in the sequel, this allows us to design improved signal sets for MBM with excellent distance properties. Consider two MBM blocks $\mathbf{x}$ and $\mathbf{x}'$, with each block formed by concatenating N MBM signal vectors, as shown below:

$$\mathbf{x} = \begin{bmatrix} \begin{bmatrix} 0 \\ \vdots \\ s_1 \\ 0 \\ \vdots \\ 0 \end{bmatrix} \\ \begin{bmatrix} 0 \\ \vdots \\ s_2 \\ 0 \\ \vdots \\ 0 \end{bmatrix} \\ \vdots \\ \begin{bmatrix} 0 \\ \vdots \\ s_N \\ 0 \\ \vdots \\ 0 \end{bmatrix} \end{bmatrix}, \quad \mathbf{x}' = \begin{bmatrix} \begin{bmatrix} 0 \\ s_1' \\ \vdots \\ 0 \\ \vdots \\ 0 \end{bmatrix} \\ \begin{bmatrix} 0 \\ s_2' \\ \vdots \\ 0 \\ \vdots \\ 0 \end{bmatrix} \\ \vdots \\ \begin{bmatrix} 0 \\ s_N' \\ \vdots \\ 0 \\ \vdots \\ 0 \end{bmatrix} \end{bmatrix}.$$

It is an obvious but important fact that any two sparse vectors are different if they either differ in the position of the non-zeros or in the value of the non-zeros even in one coordinate. If N MBM vectors are appended to form a transmission block as in $\mathbf{x}$ above, and if we consider the collection of all such blocks as the signal set, then the minimum distance is governed by those blocks which either differ in only one position or the blocks having the same support (non-zero positions) but differing in only one non-zero value, resulting in the same minimum distance as in (4). Therefore, it should be noted that, just the block transmission does not result in improved distance properties. However, imposing certain conditions on the MAP indices and the non-zeros can lead to better distance properties as we show next.

Consider the two MBM blocks $\mathbf{x}$ and $\mathbf{x}'$ as shown above. It is easy to see that the following constraints ensure higher distance between $\mathbf{x}$ and $\mathbf{x}'$:

1) The MBM blocks $\mathbf{x}$ and $\mathbf{x}'$ have higher distance between them when their supports differ in more number of positions. That is, if $\mathbf{l} = (l_1, l_2, \cdots, l_N)$ and $\mathbf{l}' = (l_1', l_2', \cdots, l_N')$ are the MAP indices of the N MBM vectors of $\mathbf{x}$ and $\mathbf{x}'$, respectively, then the distance between $\mathbf{x}$ and $\mathbf{x}'$ is increased by increasing the Hamming distance between $\mathbf{l}$ and $\mathbf{l}'$.
2) If the MBM blocks $\mathbf{x}$ and $\mathbf{x}'$ have the same support (i.e., same MAP indices), then the distance between $\mathbf{x}$ and $\mathbf{x}'$ can be increased by increasing the distance between the non-zeros of $\mathbf{x}$ and $\mathbf{x}'$. That is, if $\mathbf{s} = [s_1 s_2 \cdots s_N]^T$ and $\mathbf{s}' = [s_1' s_2' \cdots s_N']^T$ denote the vectors containing the non-zeros of $\mathbf{x}$ and $\mathbf{x}'$, then the distance between $\mathbf{x}$ and $\mathbf{x}'$ can be increased by increasing the distance between $\mathbf{s}$ and $\mathbf{s}'$, in the case when $\mathbf{x}$ and $\mathbf{x}'$ have the same support.

Note that the first condition is the result of the sparse nature of the MBM signal vectors, while the second condition is the one that is conventionally considered in the constellation design of the multidimensional coded modulation and space-time MIMO systems. In the next subsections, we show that *MAP-index coding* can be used to achieve the first condition and the *multilevel squaring construction* can be used to achieve the second condition.

C. MAP-index coding

As noted earlier, the MAP indices are the unique indices assigned to different MAPs created by the different ON/OFF combinations of RF mirrors. For an MBM system with m_{rf} RF mirrors, there are $N_m = 2^{m_{rf}}$ different MAPs and hence N_m MAP indices, which we denoted by the set $\mathcal{M} = \{0, 1, \cdots, N_m - 1\}$. The MAP index decides the position of the non-zero entry in each MBM vector. Therefore, the set of MAP indices $(l_1, l_2, \cdots, l_N)$ corresponding to the N MBM vectors of the MBM transmission block decides the positions of N non-zeros in the MBM block. If $\mathbf{l} = (l_1, l_2, \cdots, l_N)$ and $\mathbf{l}' = (l_1', l_2', \cdots, l_N')$ are the MAP index vectors of the MBM blocks $\mathbf{x}$ and $\mathbf{x}'$, respectively, then, as mentioned in the condition 1 above, the distance between $\mathbf{x}$ and $\mathbf{x}'$ can be increased by increasing the Hamming distance between $\mathbf{l}$ and $\mathbf{l}'$. Therefore, if block codes with good Hamming distance properties can be suitably adopted for selecting the N MAP indices in an MBM block, it is possible to achieve good distance properties between the MBM blocks. To this end, we present the notion of MAP-index coding [26], which can be explained as follows.

First, the elements of the MAP index set $\mathcal{M} = \{0, 1, \cdots, N_m - 1\}$ are used as labels for the N_m elements of Galois field GF(N_m). This establishes an one-to-one mapping

between the MAP indices and the elements of GF(N_m). An example mapping is shown in Table II for the case when $m_{rf} = 3$, and hence $N_m = 8$.

M1 status	M2 status	M3 status	MAP index	GF(N_m)
ON	ON	ON	0	0
ON	ON	OFF	1	1
ON	OFF	ON	2	X
ON	OFF	OFF	3	$X+1$
OFF	ON	ON	4	X^2
OFF	ON	OFF	5	X^2+1
OFF	OFF	ON	6	X^2+X
OFF	OFF	OFF	7	X^2+X+1

TABLE II: Labeling of MAP indices to elements of GF($2^{m_{rf}}$).

Then, consider an (N, K) non-binary block code on GF(N_m) with certain Hamming distance properties. The set of all N-length codewords of this (N, K) block code forms a codebook on GF(N_m) with $N_m^K = 2^{Km_{rf}}$ codewords. Since there is one-to-one mapping between the elements of GF(N_m) and $\mathcal{M}$, the codebook of the considered (N, K) block code on GF(N_m) induces an equivalent codebook on $\mathcal{M}$, with the same Hamming distance properties as that of the original block code on GF(N_m). Let $\mathcal{S}_{\text{map}}$ denote such an (N, K) codebook on $\mathcal{M}$. Also, let d_H be the minimum Hamming distance of $\mathcal{S}_{\text{map}}$. Then, any two codewords $\mathbf{l} = (l_1, l_2, \cdots, l_N)$ and $\mathbf{l}' = (l'_1, l'_2, \cdots, l'_N)$ will differ in at least d_H positions. Therefore, if the codebook $\mathcal{S}_{\text{map}}$ is used as the alphabet for N MAP indices of the MBM block, then any two blocks $\mathbf{x}$ and $\mathbf{x}'$ having different supports will differ in at least d_H positions, resulting in a distance of

$$d(\mathbf{x}, \mathbf{x}') = \sum_{i=1}^{d_H} (|s_i|^2 + |s_i|'^2). \tag{5}$$

This distance is clearly greater than the minimum distance of the conventional MBM signal set in (4) when $d_H > 1$.

Although MAP-index coding is able to increase the distances between MBM blocks with different support, in order to increase the minimum distance of the signal set, the distance between the signal vectors having the same support but differing only in non-zero values should also be increased. Therefore, for MBM blocks $\mathbf{x}$ and $\mathbf{x}'$ with the same support, the non-zero symbol vectors $\mathbf{s}$ and $\mathbf{s}'$ corresponding to $\mathbf{x}$ and $\mathbf{x}'$ should be designed such that they have certain guaranteed minimum distance between them. This leads us to multilevel squaring construction, which we present next.

D. Multilevel squaring construction

As seen in the previous subsection, when the supports of the MBM blocks $\mathbf{x}$ and $\mathbf{x}'$ overlap, the non-zeros of the two blocks $\mathbf{s}$ and $\mathbf{s}'$ should have higher distance ($\|\mathbf{s} - \mathbf{s}'\|^2$) between them to ensure higher distance between $\mathbf{x}$ and $\mathbf{x}'$. As seen in Sec. II, the squaring construction allows us to construct a set of vectors with certain assured minimum distance, starting from a set of scalars. Therefore, the squaring construction is ideally suited to construct signal constellations with good distance properties. In the present work, we use the multilevel squaring construction starting from an M-PAM alphabet and construct an N dimensional signal set $\mathcal{A}$ with good distance properties.

Figure 2 shows the tree representation of a two stage squaring construction starting from 4-PAM alphabet $\mathbb{A} = \{-3, -1, 1, 3\}$. Each stage of the squaring construction consists of two steps, viz., the set partition step followed by the Cartesian product (which we have indicated as 'squaring' in Fig. 2). In each stage of the construction, we have shown the minimum distance between the vectors of that stage. The minimum distance of the original PAM signal set is $d_{min} = 4$. Then, the squaring construction as described in Sec. II is applied on this set to get a two dimensional signal set with a minimum distance of $d_{\text{min}} = 16$. The dimension of the signal set is increased from one to two after the first stage of squaring construction. Now, the squaring construction is repeated on the resulting two dimensional signal set to obtain a four dimensional signal set with minimum distance of $d_{\text{min}} = 32$. Now, if we stop the squaring construction at this stage, we have a constellation in four real dimensions. In order to make this signal set compatible with the QAM modems, we convert this four dimensional real vectors into two dimensional complex vectors by forming complex symbols using two consecutive real symbols. For example, the two dimensional complex vectors formed using the four dimensional real vectors in Fig. 2 are given by

$$\mathcal{A} = \left\{ \begin{bmatrix} -3-3i \\ -3-3i \end{bmatrix}, \begin{bmatrix} -3-3i \\ 1+1i \end{bmatrix}, \begin{bmatrix} 1+1i \\ 1+1i \end{bmatrix}, \begin{bmatrix} 1+1i \\ -3-3i \end{bmatrix}, \begin{bmatrix} -3+1i \\ -3+1i \end{bmatrix}, \right.$$
$$\begin{bmatrix} -3+1i \\ 1-3i \end{bmatrix}, \begin{bmatrix} 1-3i \\ 1-3i \end{bmatrix}, \begin{bmatrix} 1-3i \\ -3+1i \end{bmatrix}, \begin{bmatrix} -1-1i \\ -1-1i \end{bmatrix}, \begin{bmatrix} -1-1i \\ 3+3i \end{bmatrix}, \begin{bmatrix} 3+3i \\ 3+3i \end{bmatrix},$$
$$\left. \begin{bmatrix} 3+3i \\ -1-1i \end{bmatrix}, \begin{bmatrix} -1-3i \\ -1-3i \end{bmatrix}, \begin{bmatrix} -1-3i \\ -3-1i \end{bmatrix}, \begin{bmatrix} 3-1i \\ 3-1i \end{bmatrix}, \begin{bmatrix} 3-1i \\ -1-3i \end{bmatrix} \right\}.$$

It should be noted that the distance properties of this set of two dimensional complex vectors is same as that of the set of four dimensional real vectors in Fig. 2. In the present work, the vectors of the complex constellation $\mathcal{A}$ obtained from the squaring construction are used for the non-zero parts of the MBM blocks. This makes sure that, whenever the supports of the MBM blocks overlap, the distance between the MBM blocks is high. By counting across the branches of the tree representation of the squaring construction, the number of vectors at the end of Lth stage, starting from an M-PAM alphabet, is given by

$$|\mathcal{A}| = \begin{cases} 2^L \left(\frac{M^{2^L}}{2^{2(2^L-1)}} \right) & \text{if } M \geq 4 \\ 2 & \text{if } M = 2. \end{cases} \tag{6}$$

Therefore, with $M = 2^P$, $P \geq 2$, the number of vectors in $\mathcal{A}$ is given by

$$|\mathcal{A}| = 2^{2^L(P-2)+L+2}. \tag{7}$$

It should be further noted that the L level squaring construction results in 2^L dimensional real vectors and hence $N = 2^L/2 = 2^{L-1}$ dimensional equivalent complex vectors.

E. Proposed signal set

In this subsection, we present the proposed signal set for MBM by putting together the ideas discussed so far. As seen from the previous subsections, the MAP-index coding

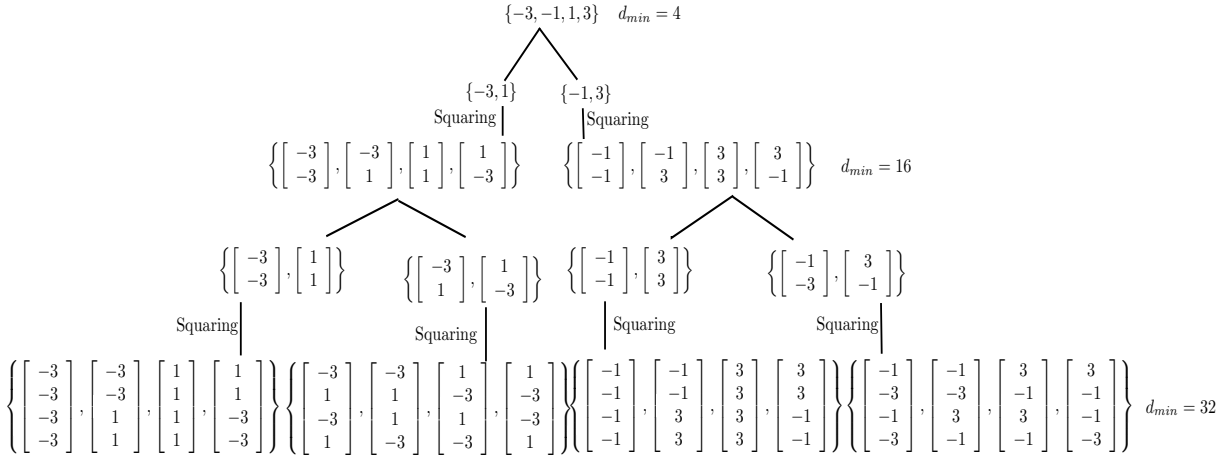

Fig. 2: Illustration of multilevel squaring construction.

results in a codebook, which we denote by $\mathcal{C}_b$, consisting of N-length codewords on $\mathcal{M}$. This codebook can be thought of as the signal set from which the MAP-index vectors $\mathbf{l}=(l_1,l_2,\cdots,l_N)$ for MBM blocks are selected. Further, the multilevel squaring construction results in a multidimensional signal set $\mathcal{A}$, whose elements are used for the non-zero part of the MBM blocks. The proposed signal set for MBM is the combination of the two signal sets $\mathcal{C}_b$ and $\mathcal{A}$, and is given by

$$\mathbb{S}=\{\mathbf{x}=[\mathbf{x}_1^T\mathbf{x}_2^T\cdots\mathbf{x}_N^T]^T \text{ s.t } (l_1,\cdots,l_N)\in\mathcal{C}_b,\ \mathbf{s}\in\mathcal{A}\}, \tag{8}$$

where $\mathbf{x}_1,\cdots,\mathbf{x}_N$ are the N MBM vectors which form the MBM block $\mathbf{x}$, $(l_1,\cdots,l_N)$ are the MAP indices of $\mathbf{x}_1,\cdots,\mathbf{x}_N$, respectively, and $\mathbf{s}=[s_1,\cdots,s_N]\in\mathcal{A}$ is such that s_i is the non-zero symbol (the source symbol) of $\mathbf{x}_i$ (the ith MBM vector of the MBM block).

Example: For a system with $N=4$, $K=2$, $m_{rf}=3$, and $M=2$, the signal set $\mathcal{A}$ consisting of 2 vectors generated by squaring construction is

$$\mathcal{A}=\left\{\begin{bmatrix}-1-1i\\-1-1i\\-1-1i\\-1-1i\end{bmatrix},\begin{bmatrix}1+1i\\1+1i\\1+1i\\1+1i\end{bmatrix}\right\}, \tag{9}$$

and the MAP-index codebook $\mathcal{C}_b$ generated by $(4,2)$ shortened Reed-Solomon code on GF(8), consisting of $2^{Km_{rf}}=2^6=64$ codewords, is given by

$$\mathcal{C}_b=\left\{\begin{bmatrix}0\\0\\0\\0\end{bmatrix},\begin{bmatrix}0\\1\\6\\3\end{bmatrix},\begin{bmatrix}0\\2\\7\\6\end{bmatrix},\begin{bmatrix}0\\3\\1\\5\end{bmatrix},\begin{bmatrix}0\\4\\5\\7\end{bmatrix},\cdots,\begin{bmatrix}7\\7\\3\\5\end{bmatrix}\right\}. \tag{10}$$

Each vector in $\mathcal{C}_b$ is a MAP-index vector, whose entries are used as the MAP-indices for the 4 MBM sub-vectors which constitute the MBM block. The MBM block is then formed by transmitting one of the vectors from $\mathcal{A}$ using one of the MAP-index vectors from $\mathcal{C}_b$. For example, if the first vector of $\mathcal{C}_b$ is used as the MAP-index vector and the first vector in $\mathcal{A}$ is to be transmitted, then the MBM transmit block corresponding to this combination is a $NN_m=32$-length signal vector given by

$$\begin{aligned}\mathbf{x}=[&(-1-i)\ 0\ 0\ 0\ 0\ 0\ 0\ 0\ (-1-i)\ 0\ 0\ 0\ 0\ 0\ 0\ 0\\&(-1-i)\ 0\ 0\ 0\ 0\ 0\ 0\ 0\ (-1-i)\ 0\ 0\ 0\ 0\ 0\ 0\ 0]^T.\end{aligned} \tag{11}$$

Likewise, if the second vector of $\mathcal{C}_b$ is used as the MAP-index vector and the second vector in $\mathcal{A}$ is to be transmitted, then the signal vector is given by

$$\begin{aligned}\mathbf{x}=[&(1+i)\ 0\ 0\ 0\ 0\ 0\ 0\ 0\ 0\ (1+i)\ 0\ 0\ 0\ 0\ 0\ 0\\&0\ 0\ 0\ 0\ 0\ 0\ (1+i)\ 0\ 0\ 0\ 0\ (1+i)\ 0\ 0\ 0\ 0]^T.\end{aligned} \tag{12}$$

The proposed MBM constellation $\mathbb{S}$ is the set of all such MBM blocks obtained by different combinations of MAP-index vectors from $\mathcal{C}_b$ and symbol vectors from $\mathcal{A}$.

The number of MBM blocks in $\mathbb{S}$ (i.e., the number of signal points in the proposed constellation) is $|\mathbb{S}|=|\mathcal{C}_b||\mathcal{A}|$. As seen before, $|\mathcal{C}_b|=N_m^K=2^{Km_{rf}}$ and $|\mathcal{A}|=2^{2^L(P-2)+L+2}$ for $P\geq 2$, and $|\mathcal{A}|=2$ for $P=1$. Therefore, the rate achieved by transmitting an MBM block from the proposed signal set $\mathbb{S}$ for $P\geq 2$ is given by

$$\begin{aligned}\eta&=\frac{1}{N}\left\{\log_2\left(2^{Km_{rf}}\cdot 2^{2^L(P-2)+L+2}\right)\right\}\\&=\frac{1}{N}\left[Km_{rf}+2^L(P-2)+L+2\right]\\&=\frac{1}{N}\left[Km_{rf}+2N(\log_2 M-2)+\log_2(2N)+2\right].\end{aligned} \tag{13}$$

For the case when $P=1$, the rate is given by

$$\begin{aligned}\eta&=\frac{1}{N}\left\{\log_2\left(2^{Km_{rf}}\cdot 2\right)\right\}\\&=\frac{1}{N}\left[Km_{rf}+1\right].\end{aligned} \tag{14}$$

For example, if $N=4$, $K=2$, $m_{rf}=2$, $M=4$, the achieved rate is

$$\begin{aligned}\eta&=\frac{1}{4}\left[2\cdot 2+2\cdot 4(\log_2 4-2)+\log_2 8+2\right]\\&=\frac{9}{4}=2.25\quad\text{bpcu.}\end{aligned}$$

Further, the minimum distance of the signal set in (8) is given by

$$d(\mathbb{S}) = \min_{\mathbf{s},\mathbf{s}' \in \mathcal{A}} \left\{ \sum_{i=1}^{d_H} (s_i^2 + s_i'^2), \|\mathbf{s} - \mathbf{s}'\|^2 \right\}, \quad (15)$$

where the first term inside the brackets is the distance between the blocks when the supports are non-overlapping and the second term corresponds to the case when the supports are overlapping.

F. The received signal

In this subsection, we present the expression for the received signal when an MBM block from the proposed signal set (8) is transmitted. We assume a frequency flat Rayleigh fading channel which remains constant for the duration of N channel uses. An MBM block transmitted in N channel uses can be written in the matrix form as an $N_m \times N$ matrix $\mathbf{X} = [\mathbf{x}_1 \cdots \mathbf{x}_N]$, such that $\text{vec}(\mathbf{X}) = \mathbf{x} \in \mathbb{S}$. The received $n_r \times N$ matrix in N channel uses is then given by

$$\mathbf{Y} = \mathbf{H}\mathbf{X} + \mathbf{N}, \quad (16)$$

where $\mathbf{H} \in \mathbb{C}^{n_r \times N_m}$ is the MBM channel matrix, whose entries are assumed i.i.d $\mathcal{CN}(0,1)$ and $\mathbf{N} \in \mathbb{C}^{n_r \times N}$ is the additive white Gaussian noise matrix with its entries being i.i.d $\mathcal{CN}(0,\sigma^2)$. The received signal in (16) can be written in vector form as

$$\mathbf{y} = (\mathbf{I} \otimes \mathbf{H})\mathbf{x} + \mathbf{n}, \quad (17)$$

where $\mathbf{y} = \text{vec}(\mathbf{Y})$, $\mathbf{x} = \text{vec}(\mathbf{X}) \in \mathbb{S}$, and $\mathbf{n} = \text{vec}(\mathbf{N})$. The maximum-likelihood (ML) detection rule for signal detection with the proposed signal set is

$$\widehat{\mathbf{x}} = \underset{\mathbf{x} \in \mathbb{S}}{\text{argmin}} \, \|\mathbf{y} - (\mathbf{I} \otimes \mathbf{H})\mathbf{x}\|^2. \quad (18)$$

IV. BER AND ASYMPTOTIC DIVERSITY ANALYSES

From (8) and (16), it can be seen that there is certain dependence in time among the transmit MBM vectors of an MBM block and that the transmit block can be written in the form of an $N_m \times N$ space time codeword. Therefore, it is of interest to study if the proposed signal set can provide any diversity gain apart from improved distance properties. To this end, in this section, we carry out the BER and asymptotic diversity analyses of MBM using the proposed signal set.

Consider two MBM blocks $\mathbf{X}^{(i)}$ and $\mathbf{X}^{(j)}$, such that $\text{vec}(\mathbf{X}^{(i)})$, $\text{vec}(\mathbf{X}^{(j)}) \in \mathbb{S}$. The pairwise error probability (PEP) between $\mathbf{X}^{(i)}$ and $\mathbf{X}^{(j)}$, given the channel $\mathbf{H}$, is the probability that $\mathbf{X}^{(i)}$ is transmitted and it is detected as $\mathbf{X}^{(j)}$ at the receiver, with the channel being known to the receiver. This probability is given by

$$\begin{aligned} \text{PEP}_{|\mathbf{H}}(\mathbf{X}^{(i)}, \mathbf{X}^{(j)}) &= \Pr\{\mathbf{X}^{(i)} \to \mathbf{X}^{(j)} | \mathbf{H}\} \\ &= \Pr\{\|\mathbf{Y} - \mathbf{H}\mathbf{X}^{(i)}\|_F^2 \leq \|\mathbf{Y} - \mathbf{H}\mathbf{X}^{(j)}\|_F^2\}, \end{aligned} \quad (19)$$

where $\|\cdot\|_F^2$ denotes the Frobinius norm of a matrix. The PEP in (19) can be simplified as [24],[25]

$$\text{PEP}_{|\mathbf{H}}(\mathbf{X}^{(i)}, \mathbf{X}^{(j)}) = Q(\sqrt{\rho D_{ij}/2}), \quad (20)$$

where $Q(\cdot)$ denotes the Q-function, $D_{ij} \triangleq \|\mathbf{H}(\mathbf{X}^{(i)} - \mathbf{X}^{(j)})\|_F^2$, and ρ is the signal-to-noise ratio (SNR) per receive branch at the receiver. The PEP in (20) can be upper bounded as

$$\text{PEP}_{|\mathbf{H}}(\mathbf{X}^{(i)}, \mathbf{X}^{(j)}) \leq \frac{1}{2} e^{-\rho D_{ij}/4}, \quad (21)$$

where we have used the inequality $Q(x) \leq \frac{1}{2}e^{-x^2/2}$. For i.i.d Gaussian channels, unconditioning the PEP over the channel results in the following inequality [24],[25]

$$\begin{aligned} \text{PEP}(\mathbf{X}^{(i)}, \mathbf{X}^{(j)}) &\leq \frac{1}{2} \left(\frac{1}{\det\left(\mathbf{I}_{N_m} + \frac{\rho}{4}(\mathbf{X}^{(i)} - \mathbf{X}^{(j)})(\mathbf{X}^{(i)} - \mathbf{X}^{(j)})^H\right)} \right)^{n_r} \\ &= \frac{1}{2} \left(\frac{1}{\prod_{r_{ij}=1}^{R_{ij}} (1 + \sigma_{r_{ij}}^2 \rho/4)} \right)^{n_r}, \end{aligned} \quad (22)$$

where $\mathbf{I}_{N_m}$ is the $N_m \times N_m$ identity matrix, $\sigma_{r_{ij}}$ is the r_{ij}th singular value of $(\mathbf{X}^{(i)} - \mathbf{X}^{(j)})$, and R_{ij} is its rank. The union bound based BER upper bound for the proposed signal set is then given by

$$\begin{aligned} \text{BER} &\leq \frac{1}{|\mathbb{S}|} \sum_{i=1}^{|\mathbb{S}|} \sum_{j=1, j\neq i}^{|\mathbb{S}|} \text{PEP}(\mathbf{X}^{(i)}, \mathbf{X}^{(j)}) \frac{d(\mathbf{X}^{(i)}, \mathbf{X}^{(j)})}{\kappa} \\ &= \frac{1}{|\mathbb{S}|} \sum_{i=1}^{|\mathbb{S}|} \sum_{j=1, j\neq i}^{|\mathbb{S}|} \frac{1}{2} \left(\frac{1}{\prod_{r_{ij}=1}^{R_{ij}} (1 + \sigma_{r_{ij}}^2 \rho/4)} \right)^{n_r} \frac{d(\mathbf{X}^{(i)}, \mathbf{X}^{(j)})}{\kappa}, \end{aligned} \quad (23)$$

where $d(\mathbf{X}^{(i)}, \mathbf{X}^{(j)})$ is the Hamming distance between the bit mappings of $\mathbf{X}^{(i)}$ and $\mathbf{X}^{(j)}$, and $\kappa = \log_2 |\mathbb{S}|$.

Theorem IV.1. *The asymptotic diversity order of MBM using the proposed signal set is n_r.*

Proof: At high SNR values, the PEP in (22) can be simplified as

$$\text{PEP}(\mathbf{X}^{(i)}, \mathbf{X}^{(j)}) \leq \left(\frac{\rho}{4}\right)^{-n_r R_{ij}} \left(\left(\prod_{r_{ij}=1}^{R_{ij}} \sigma_{r_{ij}}^2 \right)^{1/R_{ij}} \right)^{-n_r R_{ij}}. \quad (24)$$

From (22), the asymptotic diversity order of MBM using the proposed signal set is given by [24]

$$g_d = n_r \min_{i,j \neq i} R_{ij}, \quad (25)$$

where R_{ij} is the rank of the difference matrix $\Delta^{ij} = \mathbf{X}^{(i)} - \mathbf{X}^{(j)}$, where $\text{vec}(\mathbf{X}^{(i)})$, $\text{vec}(\mathbf{X}^{(j)}) \in \mathbb{S}$. The matrices $\mathbf{X}^{(i)}$ and $\mathbf{X}^{(j)}$ are $N_m \times N$ matrices with a single non-zero entry per column. The positions of the N non-zero entries are together determined by the MAP-index codeword, as discussed before. From (25), the diversity order is determined by the minimum R_{ij} among all $i, j \neq i$. Therefore, if we find two matrices $\mathbf{X}^{(i)}$ and $\mathbf{X}^{(j)}$ such that their difference $\Delta^{ij} = \mathbf{X}^{(i)} - \mathbf{X}^{(j)}$ has the minimum rank among all pairs of matrices, then that pair determines the asymptotic diversity order. To find such a pair, we note that any (N, K) codebook will contain an all-zero codeword. If the zero element of GF($2^{m_{rf}}$) is mapped to the MAP index '0', then the MAP-index codeword corresponding to the all-zero codeword is also all-zeros. This means that same

MAP is used in all the N channel uses. Consider two such transmission blocks

$$X^{(i)} = \begin{bmatrix} s_1^i & s_2^i & \cdots & s_N^i \\ 0 & 0 & \cdots & 0 \\ \vdots & & \cdots & \vdots \\ 0 & 0 & \cdots & 0 \end{bmatrix}, X^{(j)} = \begin{bmatrix} s_1^j & s_2^j & \cdots & s_N^j \\ 0 & 0 & \cdots & 0 \\ \vdots & & \cdots & \vdots \\ 0 & 0 & \cdots & 0 \end{bmatrix}.$$

Then, their difference matrix

$$\Delta^{ij} = \begin{bmatrix} \delta_1^{ij} & \delta_2^{ij} & \cdots & \delta_N^{ij} \\ 0 & 0 & \cdots & 0 \\ \vdots & & \cdots & \vdots \\ 0 & 0 & \cdots & 0 \end{bmatrix}, \tag{26}$$

where $\delta_k^{ij} = s_k^i - s_k^j$, clearly has rank one. Therefore, $\min_{i,j \neq i} R_{ij} = 1$, and hence the asymptotic diversity order of MBM with the proposed signal set is n_r. ■

The above result says that, although there is certain coding across time, the proposed signal set does not achieve transmit diversity. However, as we will see in the next section, MBM with the proposed signal set exhibits a diversity slope higher than n_r in the medium SNR regime and the asymptotic diversity order of n_r is observed only at extremely low BER values.

V. Results and Discussions

In this section, we present numerical and simulation results that illustrate that MBM with the proposed signal set achieves improved distance properties resulting in good bit error performance. We also show that the BER upper bound derived in the previous section closely matches the simulated BER at high SNR values. We use this bound to verify the analytical diversity order derived in the previous section.

Figure 3 shows the BER performance of MBM with the proposed signal set based on MAP-index coding (MIC) and squaring construction (SQ), which is abbreviated in the figure as MIC-SQ-MBM. The system considered in the figure uses $N = 4$, $K = 2$, $m_{rf} = 4$, $n_r = 4$, and achieves a rate of 2.25 bpcu. For MAP-index coding, the codebook of $(4, 2)$ shortened Reed-Solomon code on GF(2^4) is used and eight level ($2N = 8$) squaring construction is achieved starting from $M = 2$-PAM alphabet. The figure also shows the performance of conventional MBM signal set with rate 2 bpcu. The upper bounds on the BER for both the systems are also shown. From the figure it can be seen that the derived BER upper bound is close to the simulated BER at high SNR values. This is because the bound on the Q-function used for deriving the upper bound on the BER is tight for higher values of SNR. Further, it can be seen that the proposed signal set achieves superior bit error performance compared to conventional MBM signal set. For example, the proposed signal set has an SNR gain of about 7 dB at a BER of 10^{-5} compared conventional MBM signal set. A similar performance gain in favor of the proposed signal set is observed in Fig. 4 for another set of parameters. In Fig. 4, the proposed signal set uses $N = 4$, $K = 2$, $m_{rf} = 6$, $n_r = 4$ and achieves a rate of 3.25 bpcu. For MAP-index coding, the codebook of $(4, 2)$ shortened Reed-Solomon code on GF(2^6) is used and eight level squaring

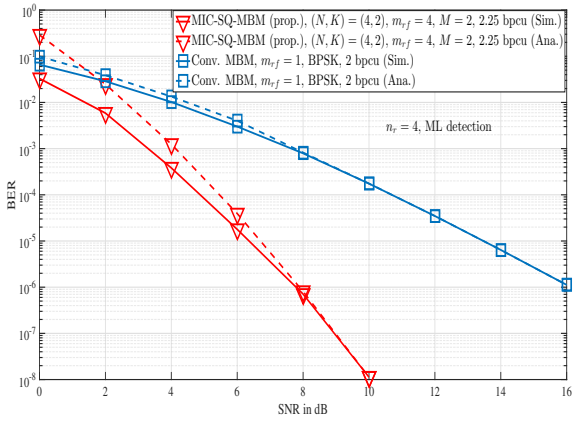

Fig. 3: BER performance of MIC-SQ-MBM (prop.) signal set with rate 2.25 bpcu and conventional MBM signal set with rate 2 bpcu. Simulation and analysis.

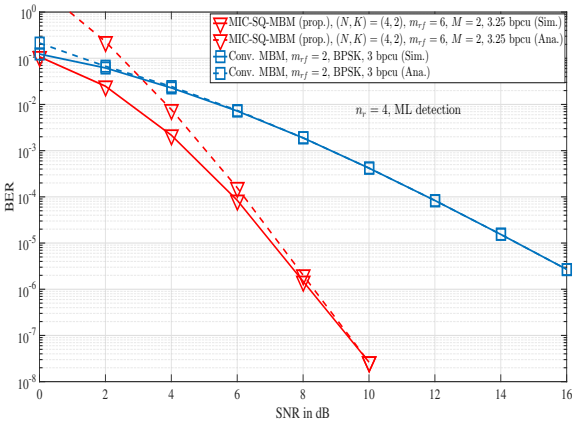

Fig. 4: BER performance of MIC-SQ-MBM (prop.) signal set with rate 3.25 bpcu and conventional MBM signal set with rate 3 bpcu. Simulation and analysis.

construction is achieved starting from $M = 2$-PAM alphabet. The performance of this MIC-SQ-MBM signal set is compared with that of conventional MBM signal set with rate 3 bpcu.

The superior BER performance of the MBM system with the proposed signal set is the result of the good distance properties achieved by the proposed signal set. The distance distributions of the proposed signal sets and conventional MBM signal sets considered in Figs. 3 and 4 are shown in Tables III and IV, respectively. From Table III, it can be seen that, the minimum distance of the conventional MBM signal set is 2, while that of MIC-SQ-MBM (proposed) signal set is 12, which is significantly higher. Further, the dominant distance in MIC-SQ-MBM signal set is 16, with 76.32 % of the signal pairs having this distance. A similar observation can be made from the Table IV where the distance distributions of conventional MBM signal set of 3 bpcu and MIC-SQ-MBM signal set of 3.25 bpcu are shown. This explains the superior performance of the proposed signal set. At this point, we make few remarks below.

Remark 1: In Theorem IV.1 in the previous section, we showed that the asymptotic diversity order of MBM with the

Distance	# pairs	% pairs
2	4	66.67
4	2	33.33

(a) MBM

Distance	# pairs	% pairs
12	15360	11.742
16	99840	76.32
20	15360	11.742
32	256	0.1956

(b) MIC-SQ-MBM

TABLE III: Distance distribution of MIC-SQ-MBM (prop.) signal set of rate 2.25 bpcu and conventional MBM signal set of rate 2 bpcu, considered in Fig. 3.

Distance	# pairs	% pairs
2	24	85.714
4	4	14.285

(a) MBM

Distance	# pairs	% pairs
12	1032192	3.0765
16	31481856	93.8346
20	1032192	3.0765
32	4096	0.0124

(b) MIC-SQ-MBM

TABLE IV: Distance distribution of MIC-SQ-MBM (prop.) signal set of rate 3.25 bpcu and conventional MBM signal set of rate 3 bpcu, considered in Fig. 4.

proposed signal set is n_r, which is same as that of MBM using conventional MBM signal set. However, in Figs. 3 and 4, even at BERs as low as 10^{-6}, the slopes of the BER curves for the proposed signal set and conventional signal set are different. Specifically, MBM with the proposed signal set is seen to exhibit a diversity slope higher than n_r. To gain more insight into this behavior, we plot the BER upper bounds of MBM using the proposed signal set for much lower BER values. The BER upper bounds for the previously considered systems in Figs. 3 and 4 are shown in Figs. 5 and 6, respectively. In Figs. 5 and 6, the bounds are plotted up to a BER of 10^{-20}. From these plots, it is evident that, although MBM using the proposed signal set initially shows a higher diversity slope, eventually the diversity slope becomes the same as that of MBM using conventional MBM signal set. For example, in Fig. 5, the curve of MBM with the proposed signal set changes the slope at about 10^{-12} BER and becomes parallel to the corresponding curve for MBM using conventional MBM signal set. This behavior can be explained as follows. As shown in the diversity analysis in Sec. IV, the slope of the BER curve in the asymptotic high SNR regime depends on the minimum rank of the difference matrices, $\mathbf{\Delta}^{ij}$s. The diversity analysis also showed that the minimum rank is always equal to one for the proposed signal set, which resulted in the conclusion that the asymptotic diversity order is n_r. The proposed signal set reduces the number of rank one difference matrices relative to the total number of possible difference matrices, which makes the effect of the minimum rank to show up only at much higher SNRs. For example, for the considered system in Fig. 5, there are 2^9 possible signal matrices $\mathbf{X}$ and hence there are $\binom{2^9}{2} = 130816$ possible difference matrices. Numerical computation of the difference matrices and their ranks reveal that there is only one difference matrix which has rank one and all other difference matrices have higher ranks. This results in the BER curve to have a slope higher than n_r in the low-to-medium SNRs and a change of slope to n_r in the high SNR regime (where the diversity slope of n_r manifests due to the effect of the presence of one difference

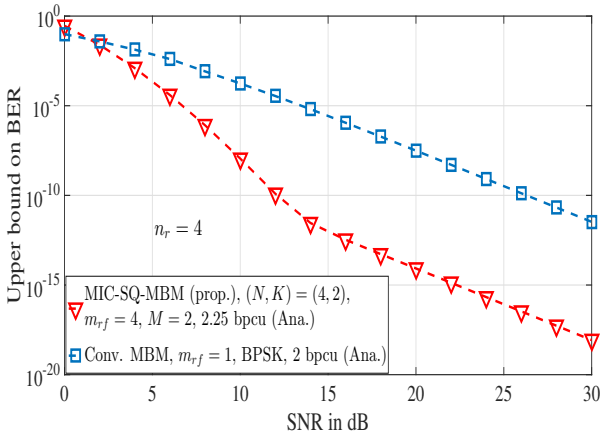

Fig. 5: BER upper bound plots of MBM using MIC-SQ-MBM (prop.) signal set and conventional MBM signal set.

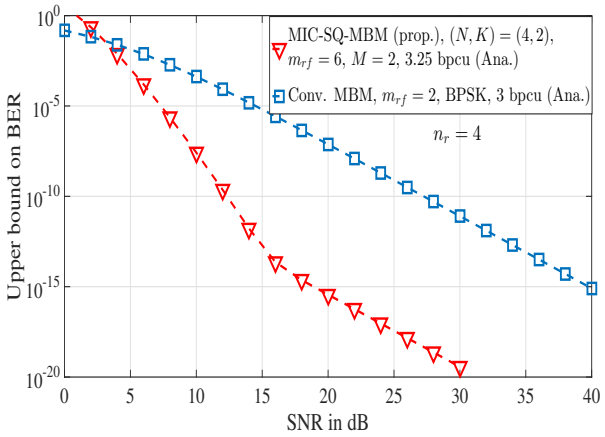

Fig. 6: BER upper bound plots of MBM using MIC-SQ-MBM (prop.) signal set and conventional MBM signal set.

matrix of rank one). Likewise, out of the $\binom{2^{13}}{2} = 33550336$ possible difference matrices in the system considered in Fig. 6, only one difference matrix has rank one. Therefore, the slope change in Fig. 6 occurs at a much lower probability of error of 10^{-15} compared to the slope change at a probability of error of 10^{-12} in Fig. 5. The observations in Figs. 5 and 6 convey the following points: i) the numerical plots of the BER upper bound validate asymptotic diversity order of n_r predicted by analysis in the previous section, and ii) the proposed signal set achieves higher than n_r diversity slope in the practical low-to-moderate SNRs of interest.

Remark 2 (Shortening of RS codes): In the discussion of the results of Figs. 3 and 4, we mentioned that a *shortened* RS code is used for MAP-index coding. In this remark, we give a brief account of the shortening of RS codes. An RS code on GF($2^{m_{rf}}$) will have a codeword length of $N = 2^{m_{rf}} - 1$ (which is not the case in Figs. 3 and 4). A shortened RS code is one in which the codeword length is less than $2^{m_{rf}} - 1$. The shortened (N, K) RS code actually uses an (N', K') RS code with $N' = 2^{m_{rf}} - 1$ and $K' = K + (N' - N)$. The shortening is done by initially padding each message of length K with $N' - N$ prepending zeros. RS encoding is done for this zero padded message to obtain a codeword with the allowed

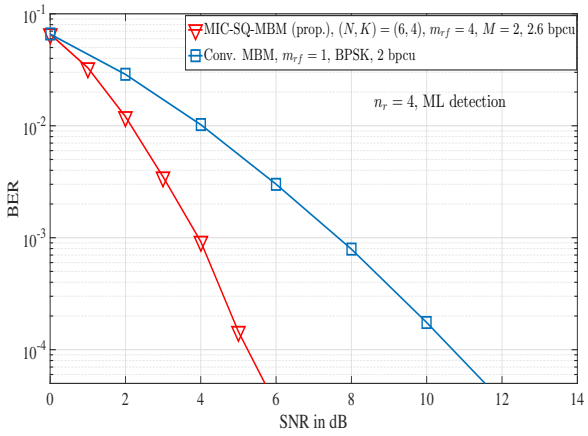

Fig. 7: BER performance of MIC-SQ-MBM (prop.) signal set with $N = 6$, $K = 4$. Performance of conventional MBM signal set is also shown for comparison.

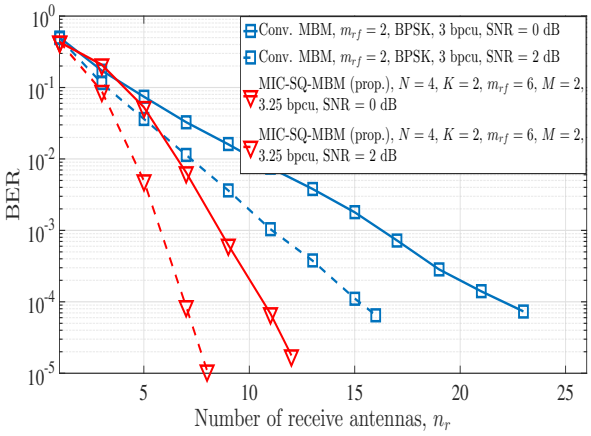

Fig. 8: BER performance of MBM using MIC-SQ-MBM (prop.) signal set as a function of number of receive antennas.

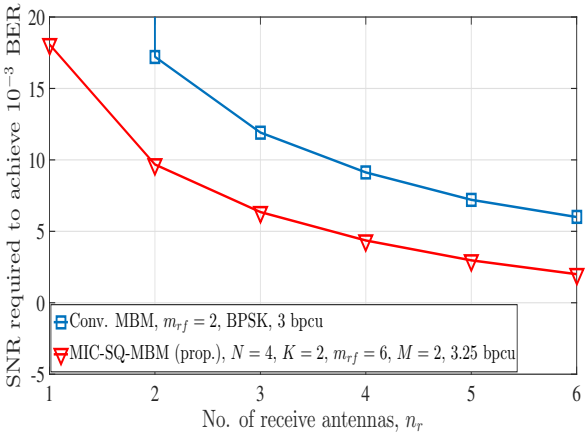

Fig. 9: SNR required to achieve a BER of 10^{-3} as a function of number of receive antennas for MBM using MIC-SQ-MBM (prop.) signal set and conventional MBM signal set.

codeword length of N'. Finally, the padded zeros are removed from the codeword along with puncturing some of the parity symbols.

In the rest of this section, we further illustrate the advantage of the proposed signal set. Figure 7 shows the BER performance of the proposed MBM signal set for $N = 6$, $K = 4$, $m_{rf} = 4$, $M = 2$, 2.6 bpcu, $n_r = 4$, and ML detection. The performance of conventional MBM signal set with $m_{rf} = 1$, BPSK, 2 bpcu, $n_r = 4$, and ML detection is also shown for comparison. From the figure, it can be seen that the proposed signal set achieves better performance compared to conventional MBM signal set by about 5 dB at 10^{-4} BER. We show the BER performance of the proposed signal set as a function of the number of receive antennas in Fig. 8. The considered system uses $N = 4$, $K = 2$, $m_{rf} = 6$, $M = 2$, and achieves a rate of 3.25 bpcu. The performance of this system is plotted as a function of the number of receive antennas at two SNR values, namely, 0 dB and 2 dB. The performance of conventional MBM signal set is also shown for comparison. From Fig. 8, it can be seen that the proposed signal set requires fewer number of receive antennas compared to conventional MBM signal set to achieve the same bit error performance. For example, to achieve a BER of 10^{-4} at an SNR of 2 dB, the proposed signal set requires about 7 receive antennas, while the conventional MBM signal set requires 15 receive antennas. It can further be seen that this gap in the required number of receive antennas widens as the required BER goes down.

In Fig. 9, the SNR required to achieve a BER of 10^{-3} for different number of receive antennas is shown for MBM with the proposed signal set (3.25 bpcu) and conventional MBM signal set (3 bpcu). It is evident from the figure that, for a given number of receive antennas, the proposed signal set achieves a BER of 10^{-3} at lesser SNR values compared to conventional MBM signal set. Figure 10 shows the BER performance of the proposed MBM constellation for $n_r = 4$ and $n_r = 16$. The performance of the conventional MBM constellation is also shown for comparison. It can be seen that the MBM performance (with proposed constellation and conventional constellation) gets significantly better for $n_r = 16$ compared to that with $n_r = 4$. This is in line with the observation in [3] where the benefits of MBM are reported to be more pronounced for a large number of receive antennas and, in many cases, the conventional constellation itself (without any channel coding) offers an acceptably low probability of error. This can be seen in Fig. 10, where the conventional constellation achieves a BER of 10^{-5} at SNRs of about 13.5 dB for $n_r = 4$ and 2.5 dB for $n_r = 16$. Figure 10 further shows that with the proposed constellation the same BER of 10^{-5} is achieved at SNRs of about 6.3 dB for $n_r = 4$ and -2.2 dB for $n_r = 16$.

In Fig. 11, we consider two MBM systems using the same number of RF mirrors ($m_{rf} = 4$) and show their BER performance as a function of E_b/N_0. The first system uses the proposed constellation with $N = 4$, $K = 2$, $M = 2$, and achieves 2.25 bpcu. The second system uses conventional MBM constellation with BPSK modulation and achieves 5 bpcu. The figure shows that the system using the proposed constellation achieves a BER of 10^{-5} at an E_b/N_0 of about 2.2 dB, whereas the system with conventional MBM constellation

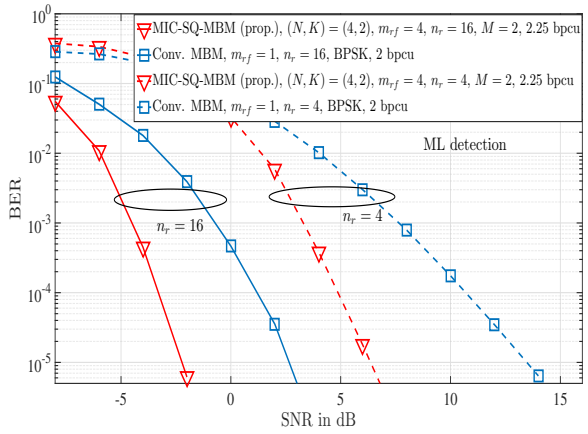

Fig. 10: BER performance of MIC-SQ-MBM (prop.) signal set and conventional MBM signal set with $n_r = 4, 16$.

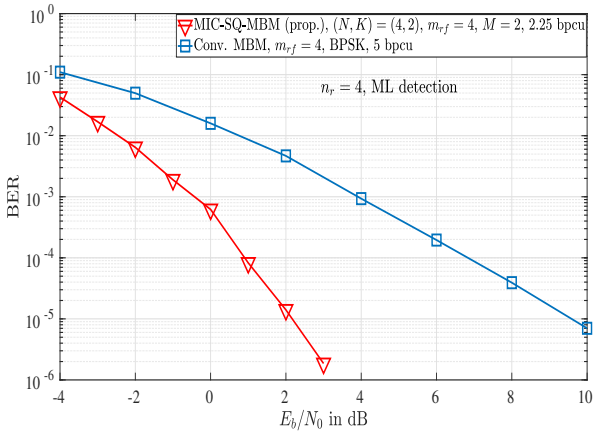

Fig. 11: BER performance comparison as a function of Eb/N_0 between the MBM systems using MIC-SQ-MBM (prop.) constellation and conventional MBM constellation, when both the systems use $m_{rf} = 4$ RF mirrors.

achieves the same BER at an E_b/N_0 of about 9.6 dB.

Figures 12a and 12b show a BER performance comparison between MBM systems using the proposed constellation and STBC systems. The MBM and STBC systems considered in the figures are closely matched in terms of their achieved rates. The considered system parameters are shown in Figs. 12a and 12b. In Fig. 12a, the MBM system has a rate of 1.75 bpcu and the STBC system has a rate of 1.5 bpcu. In Fig. 12b, the rates of both MBM and STBC systems are 2.25 bpcu. From the figures it can be seen that the MBM systems using the proposed constellation achieve better BER performance compared to the STBC systems. For example, in Fig. 12a, even with a slightly higher rate of 1.75 bpcu, the MBM system performs better by about 1 dB at 10^{-5} BER compared to the STBC system with a rate of 1.5 bpcu. In Fig. 12b, for the same rate of 2.25 bpcu, the MBM system performs better by about 5.5 dB at 10^{-5} BER. It is noted that while the considered STBC systems require $n_t = 4$ RF chains, the MBM systems require only a single RF chain.

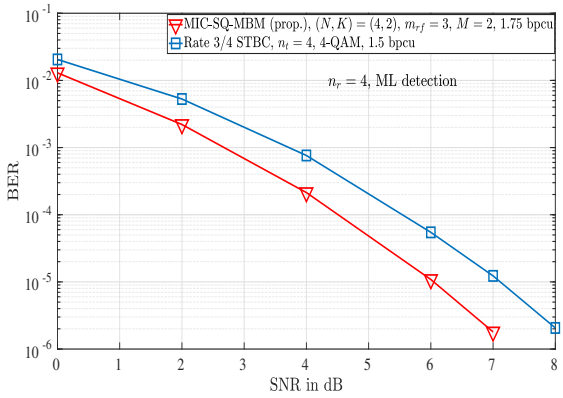

(a)

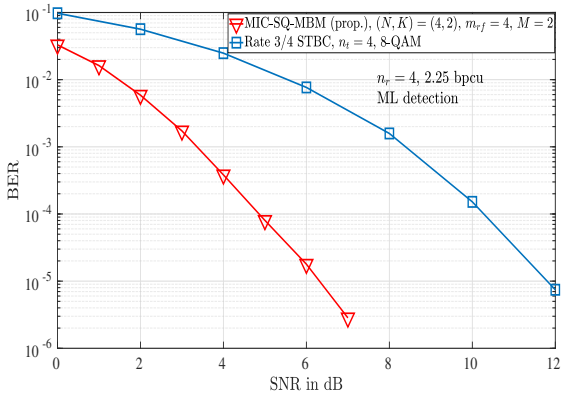

(b)

Fig. 12: BER performance comparison between MBM systems using the proposed constellation and STBC systems.

VI. Conclusions

We considered the problem of efficient constellation/signal set design for media-based modulation, and showed that block codes and squaring construction can be effectively used to design MBM signal sets with good distance properties. The proposed design approach was shown to result in MBM signal sets with good distance properties and bit error performance. Numerical and simulation results showed that the proposed MBM signal set can lead to significant advantages in terms of SNR and number of receive antennas compared to conventional MBM signal set. Through analysis and validating simulations we established that the asymptotic diversity order of the proposed signal set is the same as that of conventional MBM signal set. However, an interesting observation is that in the low-to-medium SNR regime, the proposed signal set was found to achieve a much higher diversity slope compared to that of conventional MBM signal set. This has resulted in significant SNR gains (e.g., 7 dB gain at 10^{-5} BER) compared to conventional MBM signal set. We note that the ML detection complexity grows exponentially with the block size N and hence exhaustive search becomes infeasible for large block sizes. The structured sparsity in the proposed constellation and the trellis structure of the non-zero symbols obtained by squaring construction can be exploited to design

low-complexity signal detection algorithms, which can be a potential topic future work.

REFERENCES

[1] A. K. Khandani, "Media-based modulation: a new approach to wireless transmission," in *Proc. IEEE ISIT'2013*, Jul. 2013, pp. 3050-3054.

[2] A. K. Khandani, "Media-based modulation: converting static Rayleigh fading to AWGN," in *Proc. IEEE ISIT'2014*, Jun./Jul. 2014, pp. 1549-1553.

[3] E. Seifi, M. Atamanesh, and A. K. Khandani, "Media-based MIMO: a new frontier in wireless communications," online: arXiv:1507.07516v3 [cs.IT] 7 Oct 2015.

[4] E. Seifi, M. Atamanesh, and A. K. Khandani, "Media-based MIMO: outperforming known limits in wireless," in *Proc. IEEE ICC'2016*, May 2016, pp. 1-7.

[5] Y. Naresh and A. Chockalingam, "On media-based modulation using RF mirrors," *IEEE Trans. Veh. Tech.*, vol. 66, no. 6, pp. 4967-4983, Jun. 2017.

[6] E. Basar and I. Altunbas, "Space-time channel modulation," *IEEE Trans. Veh. Tech.*, vol. 66, no. 8, pp. 7609-7614, Aug. 2017.

[7] I. Yildirim, E. Basar, and I. Altunbas, "Quadrature channel modulation," *IEEE Wireless Comm. Lett.*, vol. 6, no. 6, pp. 790-793, Dec. 2017.

[8] N. Pillay and H. Xu, "Quadrature spatial media-based modulation with RF mirrors," *IET Communications*, vol. 11, no. 16, pp. 2440-2448, 2017.

[9] B. Shamasundar, S. Jacob, T. Lakshmi Narasimhan, and A. Chockalingam, "Media-based modulation for the uplink in massive MIMO systems," *IEEE Trans. Veh. Tech.*, vol. 67, no. 9, pp. 8169-8183, Sep. 2018.

[10] A. Roy and K. J. Vinoy, "A reconfigurable screen in the antenna nearfield for media-based modulation scheme," *IEEE Intl. Microwave and RF Conf.,* Dec. 2018.

[11] M. Hasan, I. Bahceci, M. A. Towfiq, T. M. Duman, and B. A. Cetiner, "Mode shift keying for reconfigurable MIMO antennas: performance analysis and antenna design," *IEEE Trans. Veh. Tech.,* vol. 68, no. 1, pp. 320-334, Jan. 2019.

[12] C. R. Cahn, "Combined digital phase and amplitude modulation Communications," *IRE Trans. Commun. Syst.*, vol. CS-8, pp. 150-154, 1960.

[13] C. N. Campopiano and B. G. Glazer, "A coherent digital amplitude and phase modulation scheme," *IRE Trans. Commun. Syst.*, vol. CS-10, pp. 90-95, 1962.

[14] G. D. Forney, R. G. Gallager, G. R. Lang, F. M. Longstaff, and S. U. Qureshi, "Efficient modulation for band-limited channels," *IEEE J. Sel. Areas Commun.*, vol. SAC-2, no. 5, pp. 632-647, Sep. 1984.

[15] G. D. Forney, "Multidimensional constellations - part I: introduction, figures of merit, and generalized cross constellations," *IEEE J. Sel. Areas Commun.*, vol. 7, no. 6, pp. 877-892, Aug. 1989.

[16] G. D. Forney, "Multidimensional constellations - part II: Voronoi constellations," *IEEE J. Sel. Areas Commun.*, vol. 7, no. 6, pp. 941-958, Aug. 1989.

[17] L. F. Wei, "Trellis-coded modulation with multidimensional constellations," *IEEE Trans. Inform. Theory*, vol. 33, pp. 483-501, 1987.

[18] G. D. Forney, "Coset codes - part I: introduction and geometrical classification," *IEEE Trans. Inform. Theory*, vol. 34, no. 5, pp. 1123-1151, Sep. 1988.

[19] G. D. Forney, "Coset codes - part II: binary lattices and related codes," *IEEE Trans. Inform. Theory*, vol. 34, no. 5, pp. 1152-1187, Sep. 1988.

[20] H. El Gamal, G. Caire, and M. O. Damen, "On the optimality of lattice space-time (LAST) coding," in *Proc. IEEE ISIT'2004*, Jun. 2004, pp. 98.

[21] K. Raj Kumar and G. Caire, "Space-time codes from structured lattices," *IEEE Trans. Inform. Theory,* vol. 55, no. 2, pp. 547-556, Feb. 2009.

[22] O. Shalvi, N. Sommer, and M. Feder, "Signal codes: convolutional lattice codes," *IEEE Trans. Inform. Theory*, vol. 57, no. 8, pp. 5203-5226, Aug. 2011.

[23] R. A. Carrasco and M. Johnston, *Non-binary error control coding for wireless communication and data storage*, John Wiley & Sons, Nov. 2008.

[24] V. Tarokh, N. Seshadri, and A. R. Calderbank, "Space-time codes for high data rate wireless communication: performance criterion and code construction, *IEEE Trans. Inform. Theory*, vol. 44, no. 2, pp. 744-765, Mar. 1998.

[25] J. Guey, M. Fitz, M. Bell, and W. Kuo, "Signal design for transmitter diversity wireless communication systems over Rayleigh fading channels," *IEEE Trans. Commun.*, vol. 47, no. 4, pp. 527-537, Apr. 1999.

[26] B. Shamasundar, K. M. Krishnan, T. L. Narasimhan, and A. Chockalingam, "MAP-index coded media-based modulation," *IEEE Comm. Lett.*, vol. 22, no. 12, pp. 2455-2458, Dec. 2018.